Contract No:

This document was prepared in conjunction with work accomplished under Contract No. DE-AC09-08SR22470 with the U.S. Department of Energy (DOE) Office of Environmental Management (EM).

Disclaimer:

Hanford Tank Waste Disposition Integrated Flowsheet: Corrosion Specification Development Final Report

Richard B. Wyrwas

September 2018

SRNL-STI-2018-00288, Revision 0

DISCLAIMER

Printed in the United States of America

Prepared for
U.S. Department of Energy

SRNL-STI-2018-00288
Revision 0

Keywords: *Hanford, Corrosion, RPP Integrated Flowsheet, DFLAW*

Retention: *Permanent*

Hanford Tank Waste Disposition Integrated Flowsheet: Corrosion Specification Development Final Report

R.B. Wyrwas

July 2018

Prepared for the U.S. Department of Energy under contract number DE-AC09-08SR22470.

Savannah River National Laboratory™
OPERATED BY SAVANNAH RIVER NUCLEAR SOLUTIONS

REVIEWS AND APPROVALS

AUTHORS:

_____

R.B. Wyrwas, Corrosion and Material Performance, Materials Science and Technology Date

TECHNICAL REVIEW:

_____

P. Shukla, Corrosion and Material Performance, Materials Science and Technology Date

APPROVAL:

_____

B.J. Wiersma, Manager Date
Corrosion and Material Performance, Materials Science and Technology

_____

K.E. Zeigler, Manager Date
Materials Science and Technology

_____

C.C. Herman, Manager Date
Hanford Programs

ACKNOWLEDGEMENTS

This work was performed as part of a team effort at the Savannah River National Laboratory. The author would like to acknowledge and thank the following individuals for their immense assistance, collaboration, and technical support for this project. Stephen Harris from the Analytical Research and Development group for providing all the work developing statistical test matrices, results and regression analysis, and document reviews and other support that may have been minor but greatly appreciated. The author would also like to acknowledge laboratory testing and analysis, procurement, and other technical support provided by Matthew Van Swol from the Corrosion and Material Performance group, who also trained other project members on the technical aspects of the laboratory testing and monitored the test program for technical fidelity. Mitchell Vogatsky and Bryt'Ni Hill for technical support in the laboratory provided at various phases of this program. Finally, the author would like to acknowledge and thank Bruce Wiersma who structured and managed this project and provided invaluable advice and confidence through his consultation throughout the development and testing program.

EXECUTIVE SUMMARY

The Savannah River National Laboratory has developed a corrosion model to facilitate implementation of Hanford's Direct Feed Low Activity Waste flowsheet. The focus was specifically on secondary effluent waste stream compositions from the Hanford Waste Treatment and Immobilization Plant's melter off-gas treatment system returned to the Hanford Tank Farms (return stream.) The return stream compositions were predicted to contain components at relative concentrations that are significantly more corrosive toward the carbon steel waste tanks, specifically halide and sulfate anions, than the current waste compositions in the tank farms. Electrochemical tests were performed, utilizing a statistically designed matrix, to determine the corrosion chemistry limits that will mitigate pitting in the return stream. The current corrosion chemistry specifications for the Hanford Tank Farms do not mitigate for the halide concentrations that will be expected in the return stream. The model requires a 10:1 nitrite to total halide ratio, for stream compositions at a minimum of pH 10 and a maximum temperature of 40°C. The final specification may use other corrosion data that is being generated for the DST chemistry control limits to delineate between the effect of fluoride and chloride. This test program has employed statistically designed test matrices and electrochemical test methods to validate the corrosion model specifically at boundary regions to optimize corrosion control specifications.

TABLE OF CONTENTS

LIST OF TABLES viii
LIST OF FIGURES viii
LIST OF ABBREVIATIONS ix
1.0 Introduction 9
2.0 Methods 10
2.1 Statistical Methods 10
2.2 Experimental Methods 10
2.2.1 Material Tested 10
2.2.2 Sample Mounting 11
2.2.3 Electrochemical Testing and Analysis 12
2.2.3.1 Cyclic Potentiodynamic Polarization tests and classification 12
2.2.3.2 ASTM G 192 Test and Interpretation 14
3.0 Review and Discussion of Results 14
3.1 Determination of Interaction Terms and Significant Variables 15
3.2 Role of Fluoride and Variables of Lower Significance 15
3.3 Establishment of the Preliminary Boundary Model 16
3.4 Logistic Regression Analysis 17
4.0 Refinement and Final Model 17
5.0 Conclusions 22
6.0 References 23
Appendix A Test Matrices and Results 1

LIST OF TABLES

Table 1. Variables and Constants for Anticipated Stream Conditions.....10

Table 2. Chemical Composition of AAR TC 128 Steel (wt.%).....11

Table 3. Coefficients for Equation 1 fit to the Plackett-Burman test matrix results.....15

Table 4. Testing to establish margins around logistic model.....19

Table 5. Final test matrix for confirmatory testing and final refinement.....21

LIST OF FIGURES

Figure 1. Microstructure of AAR TC Steel (a) longitudinal, (b) transverse.....11

Figure 2. Cyclic Potentiodynamic Polarization Curves showing passing, failing, and borderline results..13

Figure 3. Plot of three components of the ASTM G 192 test.....14

Figure 4. Comparison of Equation 2 and Equation 3 regression analysis curves.....17

Figure 5. Margins test matrix and results plotted in relation to the p = 0.95 pitting equation and the first iteration of the boundary equation.....18

Figure 6. Design points for final test matrix. Blue triangles are for conditions where the model predicts no pitting and red triangles are for conditions where the model predicts pitting. The axes for the repective ion are taken from the row and column of the plot.....20

Figure 7. Final results for all tests and the regression of the final model.....20

Figure 8. Final model at 3 confidence limits plotted with the 87 points used in this development.....22

Figure 9. ASTM G 192 results for Test 6 from the confirmatory test matrix.....22

LIST OF ABBREVIATIONS

CPP	Cyclic Potentiodynamic Polarization
DFLAW	Direct Feed Law Activity Waste
DST	Double Shell Tank or Double Shell Tank System
EMF	Effluent Management Facility
E_{corr}	Corrosion Potential
E_{rp}	Repassivation Potential
FY	fiscal year
mV	millivolts
SRS	Savannah River Site
WTP	Waste Treatment and Immobilization Plant

1.0 Introduction

The condensate generated by treating the off-gas from the low activity waste (LAW) melter will be treated in the effluent management facility (EMF) in the Waste Treatment and Immobilization Plant (WTP) while the Direct Feed Low Activity Waste (DFLAW) flowsheet is implemented. A portion of the condensate is expected to be returned to the tank farms, while the majority will be recycled to the WTP LAW facility. The condensate is expected to be low in nitrate content, but high in halide content, i.e. fluoride and chloride, which can aggressively corrode carbon steel if not properly inhibited. The current DST corrosion specification does not include an inhibitor requirement when halides are the major aggressive ion in the waste chemistry and only provides corrosion protection from nitrate.

The Savannah River National Laboratory has conducted a test program to determine the appropriate corrosion controls needed to inhibit halide pitting corrosion of the carbon steel DSTs.[1] The testing program was conducted with oversight by the Tank Integrity Expert Panel for the Hanford Tank Farms. Electrochemical methods were utilized with prescribed analysis of the results and additional test methods to resolve ambiguous results.[2,3] Corrosion control equations used currently at the Savannah River Site (SRS) for halide control in dilute waste streams were tested prior to this development work and were determined to not be applicable for the anticipated high chloride concentrations returned to the tank farm. The SRS equations were developed at much lower concentrations of halides, less than 0.05 M total chloride; where the expected return streams from the WTP are expected to be up to 0.2 M total halide. When extrapolated above the upper limit of 0.05M of the equation, the SRS specification over-estimates the amount of nitrite needed to inhibit halide induced pitting. Unnecessarily requiring more inhibitor than needed increases operating costs and risks sending more inhibited waste back to tank farms than received for vitrification. This report describes the process used to establish a more moderate corrosion control specification to

mitigate pitting corrosion of the carbon steel waste tanks for waste streams that have an elevated chloride content with respect to the nitrate content.

2.0 Methods

2.1 Statistical Methods

The condensate generated in the WTP is anticipated to have a wide range of compositions that results from the range of compositions of LAW treated and immobilized in the DFLAW flowsheet. This range directly impacts the composition of return streams to tank farms. Based on the flowsheet model results received from WRPS and the WTP Contractor for the EMF evaporator feed and concentrate, the composition ranges in Table 1 were used for testing. These values include a ±30% of the maximum and minimum values for the aggressive species (+30%) and inhibitor species (-30%).

Experimental test matrices were formulated using statistical design. Two statistical design methods were used: a constrained Plackett-Burman[4] was employed to determine the significant main effects, while interaction terms were assumed to be negligible. Then a Box-Behnkin design[5] was used to generate the initial surface response model, e.g. a boundary equation, and successive iterations to refine the boundary. Box-Behnkin designs allow for the estimation of interaction terms, as well as quadratic terms of the significant variables. CPP tests discussed in the next section were conducted and the results were input into the regression analysis. For the purposes of the first round of data analysis (Plackett-Burman) the values determined for E_{rp}-E_{corr} were assumed to have a normal distribution. The boundary equation analysis utilized a logistic distribution on the data collected. In this case, the data was treated as either a pass or a fail based on the criteria outlined by the test protocol.

Table 1. Variables and Constants for Anticipated Stream Conditions

Independent variable			Dependent Variables	Constants	
	Minimum	Maximum	Erp (V)	Potassium (M)	0.01
Sulfate (M)	0.0	0.45	Ecorr (V)	pH	10
Chloride (M)	0.01	1.63	Erp- Ecorr (V)	Temperature (°C)	40
Fluoride (M)[a]	0.0	1.04			
Nitrite (M)	0.0	4.0			
Nitrate (M)	0.01	2.6			
Carbonate (M)[b]	0.0	0.07			
Phosphate (M)[b]	0.0	0.013			

[a] Fluoride was omitted in later test matrices due to solubility issues at high concentration.
[b] These constituents were held constant at the midpoint concentrations for the Box-Behnkin Test Matrix at 0.035M for Carbonate and 0.013M for Phosphate .

2.2 Experimental Methods

2.2.1 Material Tested

The coupons were fabricated from Association of American Railroads [(i)] Tank Car (AAR TC) 128 Steel. This steel was selected for testing since it approximates the chemistry and microstructure of UNS K02401

[(i)] American Association of Railroads, 425 3rd Street SW, Washington, DC 20024

[i.e., American Society for Testing and Materials (ASTM)[ii] A515 Grade 60 carbon steel], the steel from which some of the DSTs were fabricated.[6] The AARTC 128 steel was also selected because it was of the same vintage as the tank steel. The chemical composition of the steel is shown in Table 2. The yield strength for the material was greater than 380 MPa and the ultimate tensile strength was greater than 550 MPa. All elemental compositions except for Mn and Si meet the ASTM A515 specification. The Mn is greater than the maximum allowed of 0.9 wt.%, while the Si is less than the required range. The higher Mn could explain the higher than specified tensile properties (e.g., ultimate strength required to be between 415 MPa to 550 MPa).

Table 2. Chemical Composition of AAR TC 128 Steel (wt.%)

	C	Mn	P	S	Si	Fe
Specification	0.24 (max.)	0.9 (max.)	0.035 (max.)	0.04 (max.)	0.13 to 0.33	Balance
Measured	0.212	1.029	0.012	0.013	0.061	Balance

Figure 1 shows the microstructure of the rail car steel as exhibited in the longitudinal and transverse orientation. A banded, ferrite/pearlite matrix was observed. The transverse orientation also exhibited several inclusions, likely manganese sulfide inclusions.

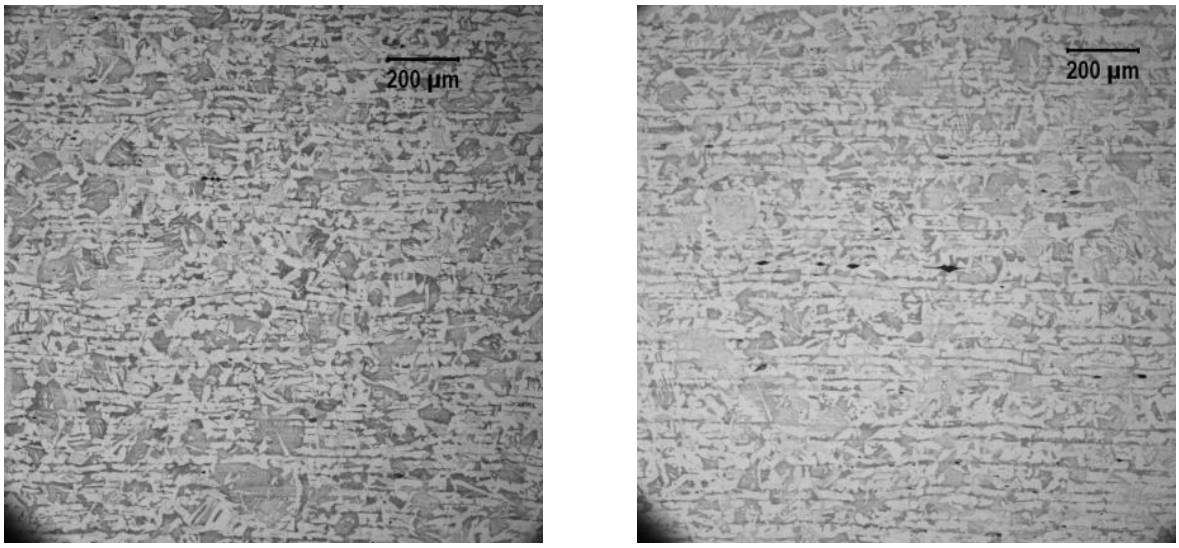

(a) (b)

Figure 1. Microstructure of AAR TC Steel (a) longitudinal, (b) transverse.

2.2.2 Sample Mounting

Carbon Steel electrodes were fabricated to an EL-400 "bullet" design. The electrode is a cylinder 1.250 in. (3.175 cm) in length, 0.188 in. (0.478 cm) diameter, with a hemi-spherical (round) end, with an area of 0.736 in^2 (4.74cm^2). The electrode was mounted using a threaded rod of 316 stainless steel sheathed in a glass tube and sealed with Teflon.

[ii] ASTM International, 100 Barr Harbor Dr., West Conshohocken, Pa 19428-2959

2.2.3 Electrochemical Testing and Analysis

2.2.3.1 Cyclic Potentiodynamic Polarization tests and classification

Cyclic Potentiodynamic Polarization (CPP) tests were performed using parameters guided by the ASTM-G 61 standard method[7] that have been specified per the Hanford corrosion testing protocol.[2] The testing protocol requires a 2-hour rest period at open circuit potential before polarizing the electrode at a scan rate of 0.167 mV/second starting at 50 mV below the measured open circuit potential, and scanning in the anodic direction until a current density of 1 mA/cm^2 is achieved. The scan potential is then stepped down at the same rate until the open circuit potential is reached. All potential measurements were made with respect to a saturated calomel reference electrode.

The CPP results are classified based on hysteresis of the curve and the difference between the corrosion potential (E_{corr}) and the repassivation potential (E_{rp}), E_{rp}-E_{corr}, if available. Figure 2 shows the classifications of the CPP curves into categories of passing, failing, and borderline test results. The CPP results in Figure 2a and 2b are considered a passing result, or a result that does not show susceptibility for pitting. Although Figure 2b, initially has a higher return current (a positive hysteresis), the repassivation potential[iii] is significantly greater than E_{corr}, such that risk of significant pit propagation is minimal by protocol definitions. Figure 2c is a mixed hysteresis result and a modified ASTM G 192 (G 192) test is performed at the same test conditions to determine the repassivation potential.[8] The G 192 test is discussed in the next section. If the G 192 results in a repassivation potential that is 200 mV above the corrosion potential (E_{corr}) then test is considered as a passing condition.[9] Figures 2d-f show a pitting or failing condition. The difference between 2b and 2d is the value of E_{rp} -E_{corr}. At times, the post-test condition of the electrode is examined and considered to help resolve CPP results. However, these observations are used to increase the confidence in the CPP classification and the electrochemical result is the data that is used to make the final determination.

[iii] The repassivation potential, sometimes referred to as the protection potential, is determined by the most noble potential at which the current of the forward scan equals the current of the reverse scan. It is straightforward to identify this potential if the current switches polarity as is the case in Figure 2b and 2d where a minimum or near-zero current is measured, similar to the feature observed near the corrosion potential.

a. Non-pitting

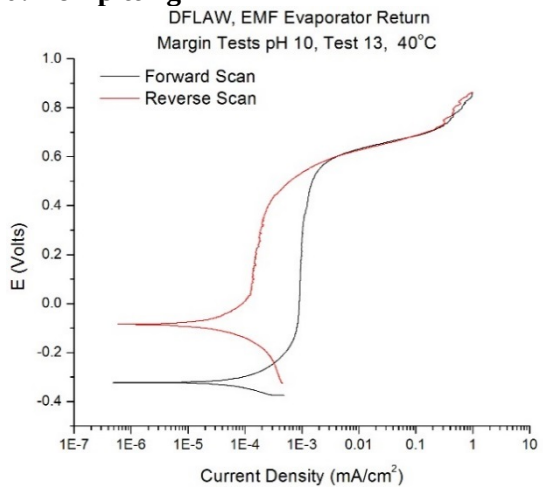

b. Passing

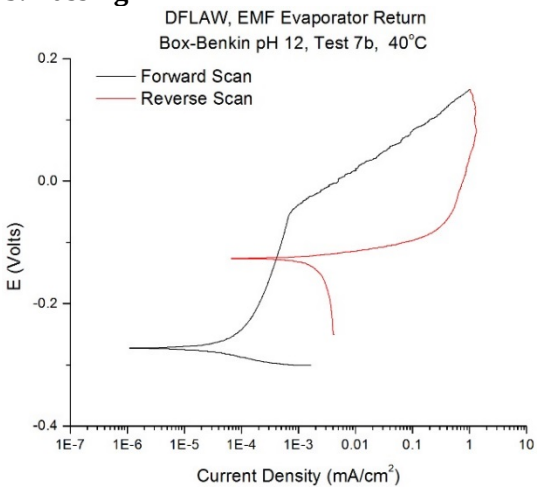

c. Borderline

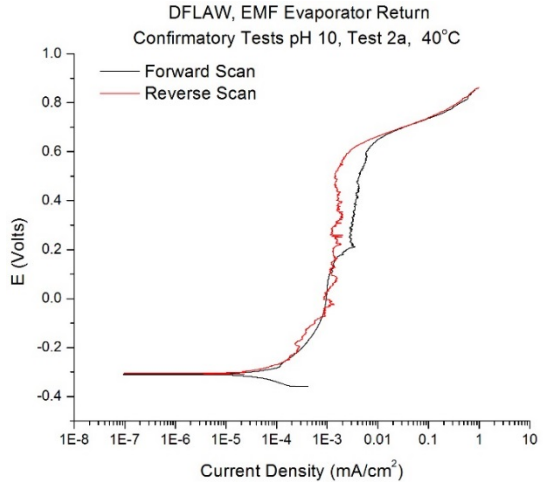

d. Pitting

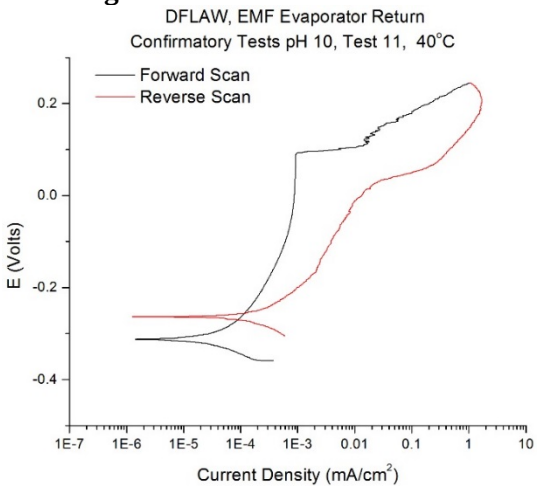

e. Pitting

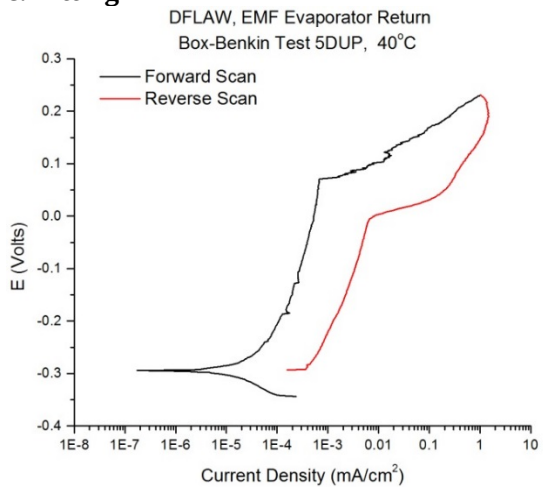

f. Pitting

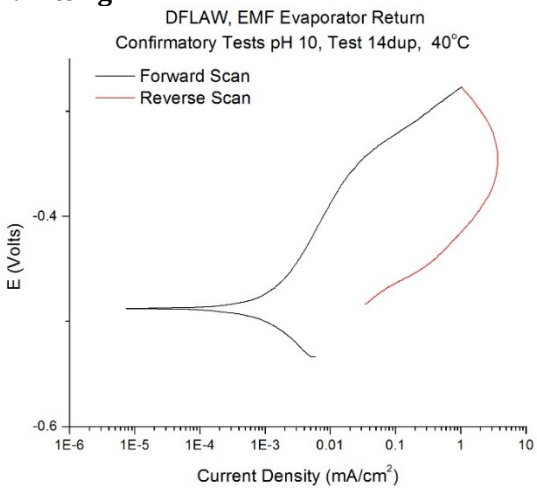

Figure 2. Cyclic Potentiodynamic Polarization Curves showing passing, failing, and borderline results.

2.2.3.2 ASTM G 192 Test and Interpretation

The ASTM G 192 consists of three successive electrochemical techniques: potentiodynamic polarization, a galvanostatic hold, and a potential step sequence. The three techniques are plotted in Figure 3. The potentiodynamic polarization (black curve) is similar to the forward scan of CPP technique and uses the same scan parameters as in the CPP test. However, instead of a potentiodynamic sweep, the apex current is held galvanostatically for 4 hours (red curve), i.e., held at constant current and adjusting the potential to maintain a constant current. At the end of the 4-hour galvanostatic hold, the technique changes to potential step, where the potential is held constant and the current is measured. Every 2 hours the potential is decreased by 25 mV, the blue line in Figure 3 shows the potential steps. This sequence continues until the measured current (dark blue line) is less than the passive current measured during potentiodynamic polarization. In this example shown in Figure 3, the passive current is about 4 E-3 mA as shown by the dashed black vertical line. In the third sequence, the potential step where the current falls below 4 E-3 mA is determined to be 485 mV. The difference for E_{rp}-E_{corr} is 826 mV, which is a category 2 or a passing result.

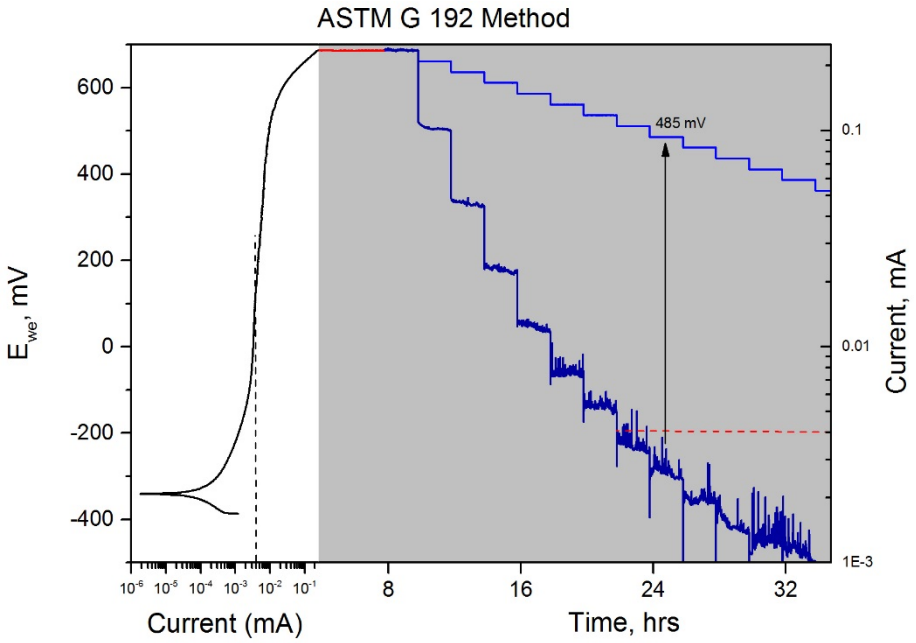

Figure 3. Plot of three components of the ASTM G 192 test.

3.0 Review and Discussion of Results

To develop a corrosion control model more suitable to protect against halide pitting from the waste, the methods discussed in the previous section were used to determine the required nitrite threshold to inhibit pitting corrosion. The initial tests results were reported at the end of fiscal year 2016 (FY16).[10] The testing employed a wider range of waste chemistry as given in Table 1 in order to optimize the full utility of the final specification. The upper and lower limits were raised or lowered an additional 30% based on whether the chemical species would be an aggressive ion or an inhibitor ion. For example, nitrate is an aggressive ion toward carbon steel, so the maximum concentration tested was 30% more than the maximum expected in WTP simulations. In contrast, nitrite is an inhibitor species and its minimum concentration was reduced 30% or to zero. The dependent variables for the system are the values measured in the electrochemical tests which are used to determine the outcome of each test. The temperature was 40°C and the solution pH 10 for the entire test matrix.

3.1 Determination of Interaction Terms and Significant Variables

The FY16 testing determined the significance of the independent variables in their ability to corrode or protect the carbon steel. A Plackett-Burman test matrix was used to make this determination and predicted that chloride is the most aggressive ion toward carbon steel and nitrite is the most effective corrosion inhibitor within the range of test compositions and under these test conditions. These results were as expected based on prior experience.[1, 11-14] The coefficients attained from the linear fit using Equation 1 are given in Table 3 were assigned negative values for aggressive ions and positive values for inhibitors ions (see Table 3). The significance of the variable, as determined by the significance level of the T Statistic (called the p-value), is also shown in Table 3 where the lower values mean that species has a significant impact on the system. Species with a T statistic value less than 0.05 were determined to be significant. Nitrate and sulfate are typically significant corrosive species in carbon steel corrosion. However, these species were statistically insignificant within this composition variable space and, although they were not included in the boundary fit equations discussed later, their significance was investigated throughout the test program.

Equation 1

$$E_{rp} - E_{corr}(V) = A + B[NO_2^-] + C[Cl^-] + D[NO_3^-] + E[F^-] + F[PO_4^{3-}] + G[SO_4^{2-}] + H[TIC]$$

Table 3. Coefficients for Equation 1 fit to the Plackett-Burman test matrix results.

Species	Coefficient	Value	Significance Level for the T Statistic
Intercept	A	0.16	0.26
Nitrite	B	0.1	0.0027
Chloride	C	-0.16	0.028
Nitrate	D	-0.051	0.22
Fluoride	E	-0.17	0.41
Phosphate	F	5.38	0.49
Sulfate	G	-0.11	0.66
Carbonate	H	0.59	0.68

3.2 Role of Fluoride and Variables of Lower Significance

It was realized that the fluoride ion was not soluble in some test formulations during laboratory testing and confirmed with thermodynamic simulations used for solution preparation guidance. The fluoride solubility was dependent on other species, such as sulfate and sodium, which added complexity to the test matrix and statistical analysis. Overall, fluoride was found to be less significant in the interaction term testing (Plackett-Burman results) and less aggressive than chloride. Based on this, the fluoride concentration was added to the chloride concentration with the intention that the final specification would be simplified for total halide control as: $[F^-]+[Cl^-]$. Other corrosion testing for the Hanford DSTs that was conducted since this testing has demonstrated that the fluoride coefficient is approximately 3 times less than that for the chloride. Thus, this approximation for the total halide would be conservative.[15] The carbonate and phosphate species were found to have little effect on the corrosion of carbon steel, so the concentration values for these ions were held constant at the respective mid-point of the range. It is important to understand this determination is specific to these series of tests and formulations. The determination described here may not hold true if the ratio of these species with respect to one another changes. This is important particularly since these ratios, e.g. range of concentrations, were established using models that may not be thermodynamically minimized.

3.3 Establishment of the Preliminary Boundary Model

The Plackett-Burman design tests determined the most significant variables were nitrite and chloride. A Box-Behnkin test matrix design was developed based on those results and yielded Equation 2 from the regression analysis.

Equation 2

$$\boldsymbol{Erp - Ecorr\ (mV)\ =\ 111\ -459\ [Cl^-]\ +171\ [NO_2^-]\ +\ 249\ [Cl^-]^2\ -\ 124\ [Cl^-][NO_2^-]}$$

The full test matrix formulations and results are included as an appendix to this report. The initial regression used the difference between the repassivation potential (E_{rp}) and the corrosion potential (E_{corr}) as the result metric. The test protocol discussed in section 2.2.3 establishes a difference of less than 200 mV (E_{rp} -E_{corr}) as failing, or at risk for pitting, and greater than 200 mV as passing, or not at risk for pitting. Using this metric, CPP results that display pitting, such as Figures 2e and 2f, would be assigned 0 mV for this result. An analysis of the results showed that there were few tests resulted in values between 0 mV and 200 mV for E_{rp} -E_{corr} (Figure 2d); a majority of the tests were either failures, e.g. 0 mV, or well above 400 mV.

Ultimately, a logistic regression analysis described in Section 3.4 was used and the CPP results were assigned as a pass for no pitting and a fail for pitting.[14] Equation 3 shows the fit using the logistic approach. The two results are compared in Figure 4 as a plot of chloride concentration versus nitrite concentration. Here any composition that is below the line is at risk for pitting and protected from pitting above the line.

Equation 3

$$\boldsymbol{[NO_2^-]\ =\ 0.805 + 4.868\ [Cl^-]}$$

In Figure 4, the data results from the SRS equation testing[1] are plotted for comparison to the preliminary equations, Equation 2 and Equation 3. The test matrix for the SRS equation were selected to have compositions that were on either side of the line and should have provided a mixture of pitting and non-pitting results. The 2015 tests were performed at 35 °C, where the lines for Equation 2 and Equation 3 were developed at 40 °C which would require more nitrite to inhibit pitting. This illustrates that this statistical approach with the logistic regression analysis is an accurate method to identify the boundary between the pitting and non-pitting compositions. The following sections will discuss the refinement of the model.

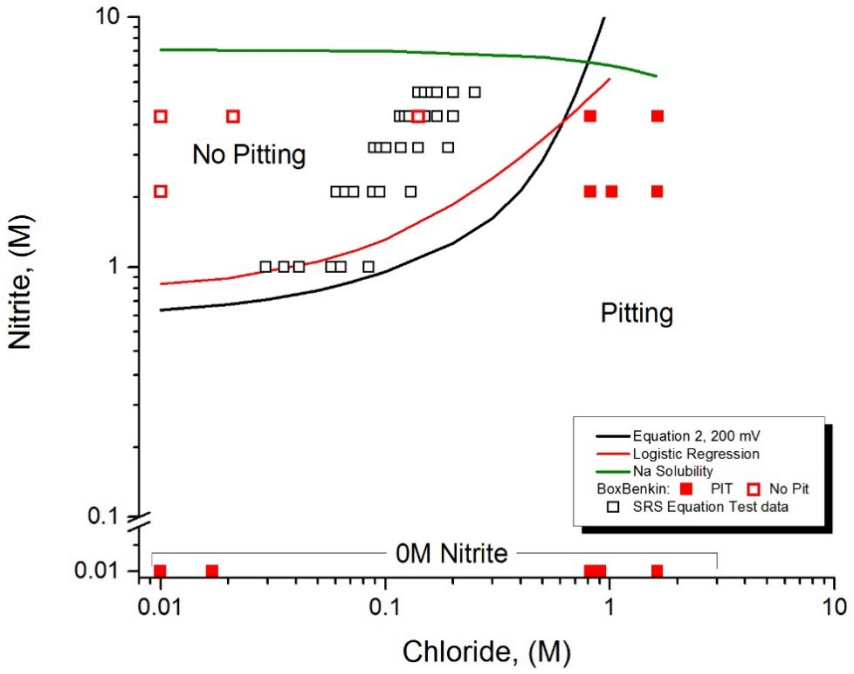

Figure 4. Comparison of Equation 2 and Equation 3 regression analysis curves.

3.4 Logistic Regression Analysis

The logistic regression analysis used the CPP test result as pass (no pitting) or fail (pitting) and gave the logistic result of 0 for non-pitting and 1 for pitting. Equation 4 gives the expression used to fit the results collected from CPP tests. For the fit plotted in Figure 3, the probability of observing pitting is set at 0.95. As later iterations refine the regression analysis, a lower confidence interval is used or conversely a higher confidence interval for no pitting, P(0), is used.

Equation 4

$$P(1) = \frac{1}{\left(1 + \mathrm{Exp}(\mathrm{Lin}[0])\right)}, \text{where} \quad \mathrm{Lin}(0) = A + B\,[Cl^-] + C[NO_2^-]$$

4.0 Refinement and Final Model

The test matrices in Section 3 used extreme values with some mid-point tests to determine the first approximation of the boundary describe by Equation 3. Successive test matrices were performed near the boundary region and used an iterative approach to refine and strengthen the boundary equation fit parameters. As discussed earlier, Equation 3 represents a pitting probability of 0.95. The plot in Figure 5 shows Equation 3 in red plotted as chloride vs. nitrite concentrations with the "No Pitting" and "Pitting" domain annotated above and below the line, respectively. The red boxes in Figure 5 are the tests from the Box-Behnkin test matrix. The probability of pitting decreases the further above the line the test composition is located, and increases below the line. Therefore, the selected test points may not appear to be equidistantly spaced across the line in Figure 5, which shows the test matrix designed to fill the gap region between 0.1 M and 1 M chloride. The test matrix is designated by the blue circles; the filled circles indicate a pitting result. Table 4 contains the formulations and results for the primary and duplicate test for each

composition. In this test matrix, there were CPP results that were split between both pitting and no pitting. In the cases where the CPP gave both results, the overall result was considered a failure and designated as such in Figure 5. Test 6 (2.4M NO_2^-, 0.35 M Cl^-) and Test 8 (3.1 M NO_2^-, 0.50 M Cl^-) are examples of the split results. This test matrix also had a number of borderline CPP, category 3, results that required the G 192 test to resolve the outcome.

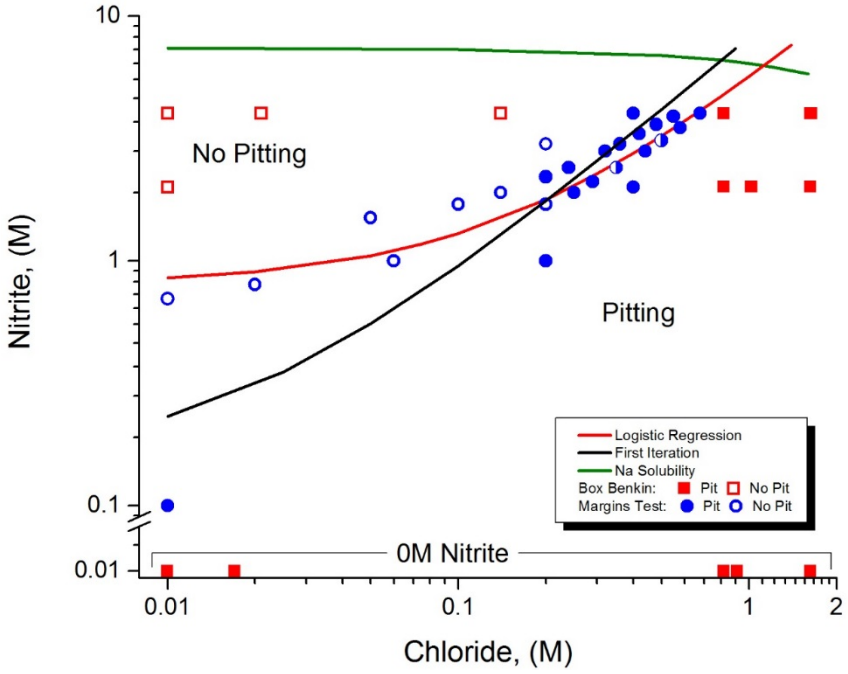

Figure 5. Margins test matrix and results plotted in relation to the p = 0.95 pitting equation and the first iteration of the boundary equation.

The first boundary line (red) was adjusted using the results from the test matrix. After incorporating these results, 6 additional tests, tests 21-26 in Table 4, were selected to increase the confidence of the regression. The second iteration of the boundary is represented in Figure 5 by the black line. This line was derived from 67 data points.

Table 4. Testing to establish margins around logistic model.

Test	$NaNO_2$	NaCl	Na_2SO_4	$NaNO_3$	Category	Logistic Test Result	Comment
	M	M	M	M	Prim/Dup		
1	0.8	0.02	0.28	2.4	1/3	0	
2	1.0	0.06	0.19	0.11	1/1	0	
3	1.7	0.20	0.29	1.9	1/1	0	
4	1.9	0.25	0.12	2.1	4/4	1	
5	2.1	0.29	0.38	2.4	4/4	1	
6	2.4	0.35	0.12	0.28	4/2	1	
7	2.8	0.44	0.20	0.66	5/5	1	
8	3.1	0.50	0.40	0.82	2/4	1	
9	3.5	0.58	0.17	0.94	5/5	1	
10	4.0	0.68	0.089	2.3	5/5	1	
11	1.5	0.05	0.36	2.3	1/1	0	G 192 pass
12	1.7	0.10	0.42	2.1	1/3	0	G 192 pass
13	1.9	0.14	0.42	2.2	1/1	0	
14	2.2	0.20	0.047	2.1	3/3	1	Did not pass G 192
15	2.4	0.24	0.086	1.7	3/3	1	Did not pass G 192
16	2.8	0.32	0.42	2.6	3/3	1	Did not pass G 192
17	3.0	0.36	0.17	0.87	5/5	1	
18	3.3	0.42	0.18	0.20	5/5	1	
19	3.6	0.48	0.33	2.3	4/4	1	
20	3.9	0.55	0..40	1.9	4/5	1	
21	0.1	0.01	0.23	1.3	5/5	1	
22	0.7	0.01	0.23	1.3	2/2	0	G 192 Pass
23	1.0	0.20	0.23	1.3	5/5	1	
24	3.0	0.20	0.23	1.3	2/2	0	G 192 Pass
25	2.0	0.40	0.23	1.3	5/4	1	
26	4.0	0.40	0.23	1.3	4/5	1	

The final test matrix is represented by the plot in Figure 6. This plot shows the relationship each of the four variables has to one another in a row-column format, and provides the prediction of pitting (red triangles) and no pitting (blue triangles). The ion concentrations are in moles/liter and the axes of each plot are identified by the row and column of the plot. For example, all the plots in column 1 have the sulfate concentration as the X-axis and the y-axis changed for each row respective to the ion- row 2 is versus chloride, etc. From these plots it can be observed that the nitrite and chloride plot is the only plot with a clear dependence between the variables. There were key test results that allowed for model adjustment: Test compositions 3 (1.1 M NO_2^-, 0.09 M Cl^-), 6 (2.7 M NO_2^-, 0.26 M Cl^-), and 8 (3.9 M NO_2^-, 0.34 M Cl^-), coincidentally, were predicted to be a non-pitting condition, but it returned a split result. This result could be reasonably expected after the model is refined as shown in Figure 7 and expressed in Equation 5 from the regression analysis from 87 points.

Equation 5

$$[NO_2^-] = 0.65 + 9.9\,[Chloride]$$

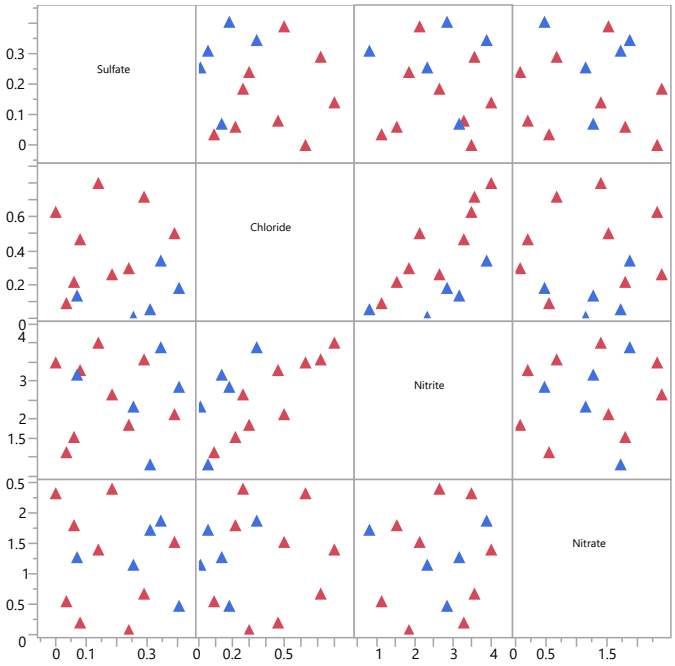

Figure 6. Design points for final test matrix. Blue triangles are for conditions where the model predicts no pitting and red triangles are for conditions where the model predicts pitting. The axes for the repective ion are taken from the row and column of the plot.

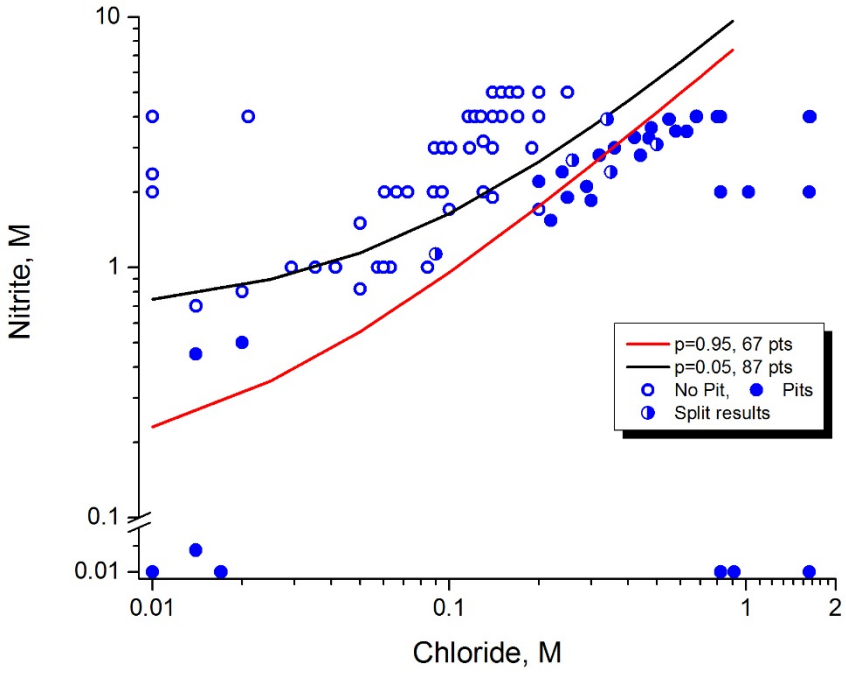

Figure 7. Final results for all tests and the regression of the final model.

Table 5. Final test matrix for confirmatory testing and final refinement.

Test	$NaNO_2$	NaCl	Na_2SO_4	$NaNO_3$	Category	Logistic Result
	M	M	M	M		
1	2.36	0.01	0.25	1.1	1/1	0
2	0.82	0.05	0.31	1.7	2/2	0
3	1.13	0.09	0.030	0.5	2/4	1
4	3.18	0.13	0.070	1.3	1/1	0
5	1.54	0.22	0.060	1.8	4/4	1
6	2.67	0.26	0.18	2.4	2/4	1
7	1.85	0.30	0.24	0.080	5/5	1
8	3.90	0.34	0.35	1.9	2/4	1
9	3.28	0.47	0.080	0.21	5/5	1
10	3.49	0.63	0.0	2.3	5/5	1
11	4.00	0.80	0.14	1.4	4/4	1
12	0.700	0.014	0.040	0.20	1/1	0
13	0.500	0.020	0.40	1.3	5/5	1
14	0.450	0.014	0.21	2.5	5/5	1

The plot in Figure 8 displays the final boundary equation at three confidence intervals for pitting, p= 0.95, p=0.5, and p=0.05. The three data points from the final confirmatory test matrix that resulted in mixed results are plotted as half-filled circles. These three points lie near the p= 0.5 confidence line. In this region of the plot, there is an equal likelihood that the test could pass or fail. However, the result for each test, primary test and duplicate test, are independent of each other, so the outcomes do not have to be 50:50 or 1:1, particularly with a small population. Likewise, it should not be surprising to get two of the same results in a small sample size. The CPP test is not necessarily random, but there are many factors to consider which may add some randomness to the system; the main one would be surface composition of the electrode such as appearance of inclusions, grain structure, and surface defects.

Figure 9 shows the results for the potentiostatic steps of the ASTM G 192 test for Test 6. The ASTM G 192 typically yields consistent results, but requires much longer times as the CPP test. In this case however, the G 192 test yielded two different results from identical test conditions. The differences can be seen easily by inspection. Figure 9A (left plot) shows the current (red trace) drops below the passivation current (5e-3 mA) in 9 potential steps and yields a repassivation potential (E_{rp}) of +520 mV, where E_{corr} is -367 mV. The difference is 887 mV, well above the 200 mV threshold and is a passing result. Figure 9B (right plot) shows a failing condition where after the forth potential step the current becomes unstable and rises above the turnaround threshold as the potential stepped down, which is classified as a failure.

This instance illustrates two key points. First, it is a good practice to collect multiple test results for CPP tests, and even more so when the test conditions maybe near a specification limit. Second, this demonstrates why it is not a good practice to operate in or near boundary limits. Operating conditions that are near the edge, may provide a false confidence of safe operation and the risk should be considered.

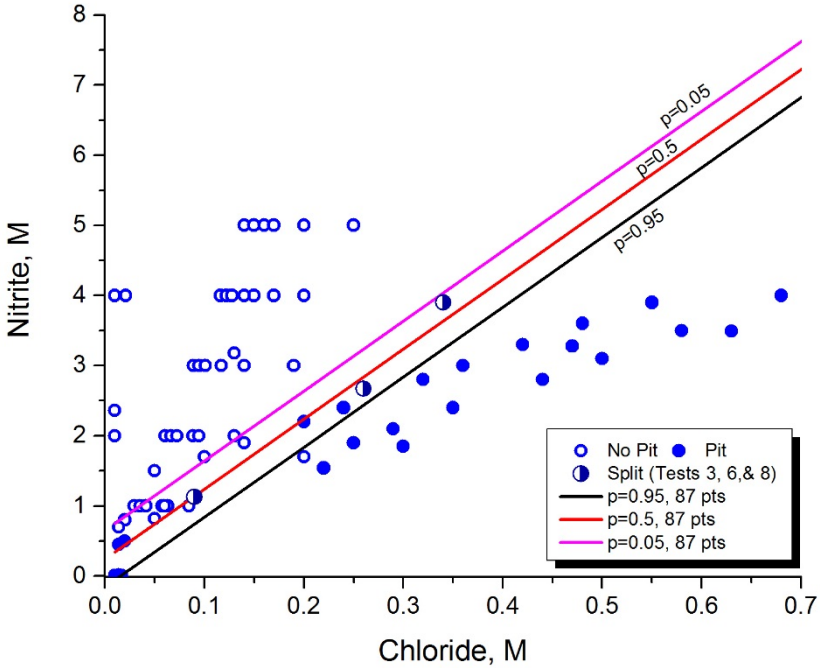

Figure 8. Final model at 3 confidence limits plotted with the 87 points used in this development.

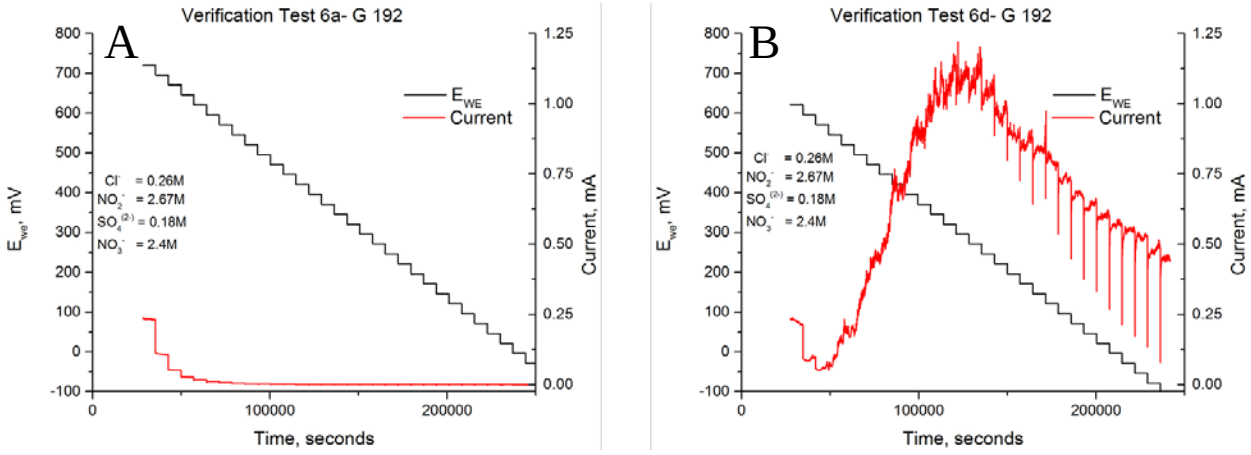

Figure 9. ASTM G 192 results for Test 6 from the confirmatory test matrix.

5.0 Conclusions

This report has presented the development of a corrosion model for an off-gas return strategy to facilitate implementation of Hanford's Direct Feed Low Activity Waste flowsheet. This testing program utilized laboratory testing along with statistical test planning and analysis to minimize the number of tests needed to determine the inhibitor limits for halide pitting control. The focus was specifically on secondary effluent waste compositions from the Hanford Waste Treatment and Immobilization Plant's melter off-gas treatment system to the Hanford Tank Farms. The stream compositions were projected to contain components at relative concentrations that are significantly more corrosive toward the carbon steel waste tanks, specifically halide and sulfate anions, than the current waste compositions in the tank farms. The current

corrosion control specifications for the Hanford Tank Farms does not control corrosion for halide concentrations that will be expected in the return stream compositions. The work presented here, and in prior reports on this project, has shown the chloride ion to be much more corrosive than the nitrate ion toward carbon steel. The halide ion has not been an issue in the Hanford Tank Farms because the nitrate levels are so much higher than the free chloride and fluoride that the inhibitor requirements for nitrate have been effective for halide. There are no processes in tank farms that change the ratio of nitrate (NO_3^-) to halide. The vitrification process will change the ratio so there is a need to update the tank farms corrosion specification to incorporate halides.

This project employed statistically designed test matrices and electrochemical test methods to validate the corrosion model specifically at boundary regions to optimize corrosion control specifications. The results have determined that nitrite (NO_2^-) in an effective inhibitor for high halide stream compositions at pH 10 and 40°C. Using the statistical iterations from 87 unique data points, the final control model as defined by Equation 5 requires a 10:1 nitrite to total halide ratio to inhibit pitting corrosion. This result should be used as the technical basis underpinning any changes to the operating specifications at the Hanford tank farms for halide corrosion control while considering other species in the waste tank, e.g., this is not a stand-alone specification. The final specification may use other corrosion data that is being generated for the DST chemistry control limits to delineate between the effect of fluoride and chloride. This final result can be incorporated in to the modeling programs to better understand the requirements for the recycle and return strategies of the flowsheet and will ultimately need to be used as part of a new specification for the tank farm.

6.0 References

1. R.B. Wyrwas, “SRNL Report for the Tank Waste Disposition Integrated Flowsheet: Corrosion Testing,” SRNL-STI-2015-00506, September 2015.
2. T.M. Martin, T. M., “Subject: Expert Panel Oversight Committee August 2014 Meeting Outcomes”, RPP-ASMT-59979, Rev. 0, September 30, 2014.
3. R. B. Wyrwas, B. J. Wiersma, S. T. Arm, K.D. Boomer, A. J. Kim, “Development of a Corrosion Control Program for Hanford Waste Treatment Plant Recycle Strategy” In CORROSION 2018. NACE International, 2018. Or see: Wiersma, B., and Wyrwas, R. "Development of a Corrosion Control Program for Hanford Waste Treatment Plant Recycle Strategy". SRNL-STI-2017-00664. doi: https://www.osti.gov/servlets/purl/1437568
4. R.L. Plackett and J.P. Burman, "The Design of Optimum Multifactorial Experiments", Biometrika 33 (4), pp. 305–25, June 1946.
5. G.E Box,. and D.W. Behnken, 1960. Some new three level designs for the study of quantitative variables. Technometrics, 2(4), pp.455-475.
6. G. L. Edgemon, V. S. Anda, H. S. Berman, M. E. Johnson, and K. D. Boomer, Corrosion: March 2009, Vol. 65, No. 3, pp. 163-174.
7. ASTM G 61, “Standard Test Method for Conducting Cyclic Potentiodynamic Polarization Measurements for Localized Corrosion Susceptibility of Iron-, Nickel-, or Cobalt-Based Alloys,” ASTM International, West Conshohocken, PA, 2014.
8. ASTM G192-08, “Standard Test Method for Determining the Crevice Repassivation Potential of Corrosion-Resistant Alloys Using a Potentiodynamic-Galvanostatic-Potentiostatic Technique”, ASTM International, West Conshohocken, PA, 2014.
9. D. C. Silverman, Corrosion 98, Paper No. 299, NACE International, Houston, TX, 1998.
10. R.B. Wyrwas, *Tank Waste Disposition Integrated Flowsheet: Corrosion Specification Development FY 16 Interim Report*. SRNL-RP-2016-00633, doi:. https://www.osti.gov/servlets/purl/1431096

11. P. E.Zapp, “Recommended Nitrite Limits for Chloride and Sulfate in ESP Slurries”, WSRC-TR-94-0250, June 6, 1994.
12. E. N. Hoffman, “Testing Vapor Space and Liquid-Air Interface Corrosion In Simulated Environments of Hanford Double-Shelled Tanks,” SRNL-STI-2011-00494, September 2011.; E. N. Hoffman, B. L. Garcia-Diaz, and T. B. Edwards, “Probability Based Corrosion Control for Liquid Waste Tanks – Part III”, SRNL-STI-2010-00246, September 2010.
13. J. W. Congdon and J. S. Lozier, “Inhibition of Washed Sludge with Sodium Nitrite”, DPST-87-379, April 7, 1987.
14. P. E. Zapp, and T.B. Edwards, “Statistical analysis of inhibitor concentrations for radioactive waste in carbon steel tanks.” No. WSRC-MS-93-492; CONF-940222-4. Westinghouse Savannah River Co., Aiken, SC (United States), 1993.
15. R.E. Fuentes, P.K. Shukla, B. Peters, and D. A. Hitchcock, “Hanford Double Shell Waste Tank Corrosion Studies – Final Report FY2018, *In preparation*.

Appendix A Test Matrices and Results

Table A- 1. Placket-Burman Test Matrix Compositions and CPP Results.

Test	NaF	NaCl	$NaNO_2$	Na_2SO_4	Na_3PO_4	Na_2CO_3	$HNaCO_3$	$NaNO_3$	CPP Result
	M	M	M	M	M	M	M	M	
1	0	0.01	0	0	0	0	0	0	1
2	0.9	0.01	0	0	0.013	0	0	0	1
3	0.9	0.01	0	0	0	0.0545	0.0156	0	1
4	0	0.01	4	0	0.013	0.0469	0.0231	0	0
5	0.13	0.01	4	0	0	0	0	2.59	0
6	0.011	0.01	4	0	0	0.0553	0.0147	2.59	0
7	0	1.63	0	0	0	0	0	0	1
8	0	1.63	0	0	0.013	0.0463	0.0237	0	1
9	0	1.63	0	0	0.013	0.049	0.0211	2.59	1
10	0.1	1.63	4	0	0.013	0	0	2.59	0
11	0.007	0.01	0	0.65	0	0.535	0.0164	0	1
12	0	0.01	0	0.65	0.013	0	0	2.59	1
13	0	0.01	0	0.65	0.013	0.046	0.0241	2.59	1
14	0	0.01	4	0.65	0.013	0	0	0	0
15	0	1.63	0	0.65	0	0.0573	0.0126	2.59	1
17	0	1.63	4	0.45	0.013	0.0417	0.0285	0	0
18	0.2	0.82	2	0	0.0065	0.0242	0.0119	1.29	1
19	0	0.82	2	0.325	0.0065	0.0232	0.035	1.29	1
20	0	0.01	0	0.45	0.013	0	0	2.59	1
21	0	0.01	0	0.45	0.013	0.046	0.0241	2.59	1
22	0	0.01	4	0.45	0.013	0	0	0	0
23	0	1.63	0	0.45	0	0.0573	0.0126	2.59	1
24	0	1.63	4	0.45	0	0	0	0	0
25	0	1.63	4	0.45	0.013	0.0417	0.0285	0	0
26	0	0.82	2	0.23	0.0065	0.0232	0.0119	1.29	1

Table A- 2. Box-Behnkin Test Matrix Compositions and CPP Results.

Test	NaCl	$NaNO_2$	Na_2SO_4	Na_3PO_4	Na_2CO_3	$HNaCO_3$	$NaNO_3$	CPP Result
	M	M	M	M	M	M	M	
1	0.01	2	0.225	0.0065	0.0230	0.0119	2.6	0
2	0.82	0	0.225	0.0065	0.0190	0.0160	2.6	1
3	0.01	0	0	0.0065	0.0147	0.0202	0.01	1
4	0.82	0	0	0.0065	0.0242	0.0110	1.305	1
5	0.82	4	0	0.0065	0.0228	0.0123	1.305	1
6	0.01	2	0.225	0.0065	0.0230	0.0121	0.01	0
7	0.82	4	0.225	0.0065	0.0225	0.0125	0.01	1
8	0.82	2	0	0.0065	0.0240	0.0110	0.01	1
9	0.82	0	0.45	0.0065	0.0239	0.0111	1.305	1
10	0.82	2	0.225	0.0065	0.0235	0.0116	1.305	1
11	0.82	2	0.45	0.0065	0.0227	0.0121	0.01	1
12	0.01	4	0.45	0.0065	0.0215	0.0135	0.01	0
13	1.63	2	0.45	0.0065	0.0225	0.0125	1.305	1
14	1.63	2	0.225	0.0065	0.0180	0.0168	0.01	1
15	1.63	0	0.225	0.0065	0.0242	0.0108	1.305	1
16	0.01	2	0	0.0065	0.0242	0.0108	1.305	0
17	1.63	4	0.45	0.0065	0.0211	0.0138	0.01	1
18	0.82	2	0.225	0.0065	0.0235	0.0116	1.305	1
19	0.01	0	0.225	0.0065	0.0231	0.0118	1.305	1
20	0.82	2	0.45	0.0065	0.0220	0.0132	2.6	1
21	0.82	2	0	0.0065	0.2400	0.0113	2.6	1
22	0.82	0	0.225	0.0065	0.0220	0.0127	0.01	1
23	0.01	4	0	0.0065	0.0220	0.0130	2.6	0
24	0.01	4	0.225	0.0065	0.0218	0.0131	1.305	0
25	1.63	2	0.225	0.0065	0.0225	0.0126	2.6	1
26	0.82	2	0.225	0.0065	0.0235	0.0116	1.305	1
27	0.01	2	0.45	0.0065	0.0227	0.0123	1.305	0
28	1.63	2	0	0.0065	0.0239	0.0123	1.305	1
29	-	-	-	-	-	-	-	
30	0.01	6	0	0.0065	0.035		0	0
31	1.64	4	0	0.0065	0.035		0	1
32	1.64	6	0	0.0065	0.035		0	1
33	1.64	4	0	0.0065	0.035		0	1
34	1.64	6	0	0.0065	0.035		2.6	1

Table A- 3. Bi-variate Margins Test Matrix, and CPP Results.

Test	NaCl	$NaNO_2$	Na_2SO_4	Na_3PO_4	Na_2CO_3	$HNaCO_3$	$NaNO_3$	CPP Result
	M	M	M	M	M	M	M	
1	0.02	0.8	0.28	0.0065	0.0238	0.0113	2.416	1
2	0.06	1	0.185	0.0065	0.0224	0.0126	0.111	0
3	0.2	1.7	0.293	0.0065	0.0233	0.0117	1.939	0
4	0.25	1.9	0.115	0.0065	0.0238	0.0112	2.095	1
5	0.29	2.1	0.382	0.0065	0.0223	0.0127	2.434	1
6	0.35	2.4	0.123	0.0065	0.0236	0.0114	0.281	1
7	0.44	2.8	0.198	0.0065	0.0233	0.0117	0.664	1
8	0.5	3.1	0.4	0.0065	0.0221	0.0129	0.819	1
9	0.58	3.5	0.174	0.0065	0.0227	0.0123	0.936	1
10	0.68	4	0.089	0.0065	0.0213	0.0137	2.285	1
11	0.05	1.5	0.361	0.0065	0.0231	0.0119	2.255	0
12	0.1	1.7	0.423	0.0065	0.0228	0.0122	2.087	0
13	0.14	1.9	0.421	0.0065	0.0225	0.0125	2.223	0
14	0.2	2.2	0.047	0.0065	0.0238	0.0112	2.12	1
15	0.24	2.4	0.086	0.0065	0.0237	0.0113	1.669	1
16	0.32	2.8	0.419	0.0065	0.0211	0.0139	2.583	1
17	0.36	3	0.171	0.0065	0.0232	0.0118	0.872	1
18	0.42	3.3	0.184	0.0065	0.0232	0.0118	0.197	1
19	0.48	3.6	0.331	0.0065	0.0208	0.0144	2.257	1
20	0.55	3.9	0.397	0.0065	0.0204	0.0149	1.907	1
21	0.01	0.1	0.225	0.0065	0.0230	0.0117	1.29	1
22	0.01	0.7	0.225	0.0065	0.0235	0.0115	1.29	1
23	0.2	1	0.225	0.0065	0.0233	0.0113	1.29	1
24	0.2	3	0.225	0.0065	0.0225	0.0121	1.29	1
25	0.4	2	0.225	0.0065	0.0235	0.0115	1.29	1
26	0.4	4	0.225	0.0065	0.0230	0.0118	1.29	1

Table A- 4. Confirmatory Test Matrix Compositions and CPP Results.

Test	NaCl	$NaNO_2$	Na_2SO_4	Na_3PO_4	Na_2CO_3	$HNaCO_3$	KNO_3	$NaNO_3$	CPP Result
	M	M	M	M	M	M	M	M	
1	0.01	2.36	0.25	0.0065	0.0233	0.0117	0.01	1.13	0
2	0.05	0.82	0.31	0.0065	0.0236	0.0114	0.01	1.73	0
3	0.09	1.13	0.03	0.0065	0.0233	0.0117	0.01	0.53	1
4	0.13	3.18	0.07	0.0065	0.0235	0.0116	0.01	1.26	0
5	0.22	1.54	0.06	0.0065	0.0240	0.0108	0.01	1.79	1
6	0.26	2.67	0.18	0.0065	0.0230	0.0124	0.01	2.39	1
7	0.3	1.85	0.24	0.0065	0.0230	0.0119	0.01	0.07	1
8	0.34	3.9	0.35	0.0065	0.0210	0.0145	0.01	1.86	1
9	0.47	3.28	0.08	0.0065	0.0235	0.0114	0.01	0.2	1
10	0.63	3.49	0	0.0065	0.0225	0.0125	0.01	2.32	1
11	0.8	4	0.14	0.0065	0.0220	0.0131	0.01	1.39	1
12	0.014	0.7	0.04	0.0065	0.0220	0.0133	0.01	0.19	0
13	0.02	0.5	0.4	0.0065	0.0230	0.0117	0.01	1.29	1
14	0.014	0.24	0.21	0.0065	0.0240	0.0109	0.01	2.49	1
15	0.014	0.45	0.21	0.0065	0.0240	0.0109	0.01	2.49	1

Distribution:

Name:	Organization:
K. E. Zeigler	SRNL
B. J. Wiersma	SRNL
R. B. Wyrwas	SRNL
C.S. Lewis	SRNL
P.K. Shukla	SRNL
R.E. Fuentes	SRNL
M. E. Stone	SRNL
J. R. Pelfrey	SRNL
C. C. Herman	SRNL
H. H. Burns	SRNL
R. B. Wyrwas	SRNL
S. T. Arm	WRPS
J.G. Reynolds	WRPS
J. Colby	WRPS